

A NUMERICAL PROCEDURE FOR THE ASSESSMENT OF HIGHWAY BRIDGES IN SEISMIC AREA

D. Cardone¹, G. Perrone² and M. Dolce³

^{1,2}DiSGG, University of Basilicata
Viale dell'Ateneo Lucano, 85100 Potenza, Italy
donatello.cardone@unibas.it, giuseppe.perr@alice.it

³ Dept. Of Civil Protection
Via Vitorchiano 4, Roma, Italy
mauro.dolce@protezionecivile.it

Keywords: Bridge Assessment, Seismic Vulnerability and Risk, Direct Displacement-based Design, Capacity Spectrum Method, Fragility Curves.

Abstract. *A numerical procedure for the evaluation of the seismic vulnerability and seismic risk of highway bridges is proposed. It combines elements from the Direct Displacement-based design method and the Capacity Spectrum Method. First, the seismic resistance of each structural subsystem (i.e. pier/abutment + bearing/seismic devices) is determined by conducting a pushover analysis, tracking the formation of flexural plastic hinges or brittle shear failures in the piers, the attainment of the maximum strength/deformation capacity in the bearing/seismic devices, unseating of simply supported spans, degradation due to P-Δ effects, etc.. The contributions of each structural subsystem are then properly assembled to provide the Pushover Curve of the bridge as a whole, both in the longitudinal and transversal direction. A number of performance levels (i.e. damage states) are then identified, for both piers and devices, and reported on the Pushover Curve of the bridge. For each of them, the equivalent viscous damping is computed and a series of normalized high-damping elastic response spectra (Demand Curves) are derived. The Pushover Curve is then step-by-step converted into an equivalent SDOF Adaptive Capacity Curve, based on the actual deformed shape of the bridge at each analysis step. The Adaptive Capacity Curve is intersected with the Demand Curves, to provide an estimate of the median threshold values of the Peak Ground Acceleration (PGA_{PL}) associated to each performance level. Based on the PGA_{PL} values thus obtained, fragility curves (seismic vulnerability) and annual probabilities of exceedance (seismic risk), for a bridge located in a given site, are obtained. Finally, the method gives the possibility to consider possible modifications of strength and ductility due to decay of materials and/or rehabilitation interventions and/or seismic retrofit interventions. In this paper, the main aspects of the proposed assessment procedure are outlined. Two case studies are then presented, involving two different types of existing bridges. Finally, a comparison with the results of accurate nonlinear dynamic analyses is carried out, showing a good accuracy in the predictions of the proposed procedure.*

1 INTRODUCTION

Bridges and viaducts are the critical elements of a road network, due to their own characteristics and the considerable consequences, in terms of both repair costs and transportation problems implied by their degradation and damage. Besides the progressive decay of the structure, severe damage can occur due to an earthquake.

Recent earthquakes [1] have repeatedly demonstrated the seismic vulnerability of existing bridges, often designed in the '60-'70, based on low lateral force levels and with a lack of attention to design details. Moreover, the slow degradation of the bridge structures can significantly change their strength and ductility, thus increasing their seismic vulnerability.

In Italy, a new seismic zonation enforced in 2003 [2] emphasises the urgent need for seismic retrofit for existing bridges.

The above considerations call for the development of advanced tools for the seismic assessment of highway bridges, able to define the seismic risk associated with given performance levels, in order to make a rational decision about the need of retrofitting or replacing an existing bridge.

The SAGGI (Advanced Systems for the Global Management of Infrastructures) research project, funded by the Italian Ministry for the University and the Research (MUR) and led by the Italian Highway Company (Autostrade per l'Italia SpA), is aimed at developing an integrated system for the effective management of the Italian motorway network. The DiSGG of the University of Basilicata is involved in SAGGI, to deal with all the seismic aspects of the project. The final objective of the DiSGG activity is to develop a tool able to evaluate the seismic risk associated to the structures under consideration in different conditions: (i) as built, (ii) taking account of the current degradation state, (iii) taking account of the natural evolution of the decay process and programmed maintenance and/or seismic upgrading measures.

In this paper the background and the implementation of the proposed procedure for the seismic assessment of bridges is presented. Particular attention is focused on the part relevant to the evaluation of the seismic vulnerability and risk. As a preliminary verification, the proposed procedure is then applied to a number of existing bridges and the results compared to those provided by nonlinear time-history analyses.

2 SEISMIC RISK ASSESSMENT PROCEDURE

The proposed procedure for the evaluation of the vulnerability and seismic risk of bridge structures combines elements from the Direct Displacement-Based Design (DDBD) Method [3] and an "adaptive" revision of the Capacity Spectrum Method (CSM) [4]. It is based on the pushover analysis for the characterization of the seismic resistance of the structure. The final output of the procedure are a series of "fragility curves", which describe the seismic vulnerability of the bridge under a probabilistic perspective. The seismic risk is expressed by the probability of exceedance of given damage states, conditioned on the site return period hazard.

The procedure has been developed in Visual Basic environment. It exploits an electronic spreadsheet as graphical interface.

Figure 1 shows the flowchart of the proposed procedure. Basically, it consists of three phases: (i) derivation of pushover curves, taking into account possible structural decay scenarios, (ii) evaluation of the structural vulnerability and seismic risk and (iii) design and implementation of possible retrofit measures.

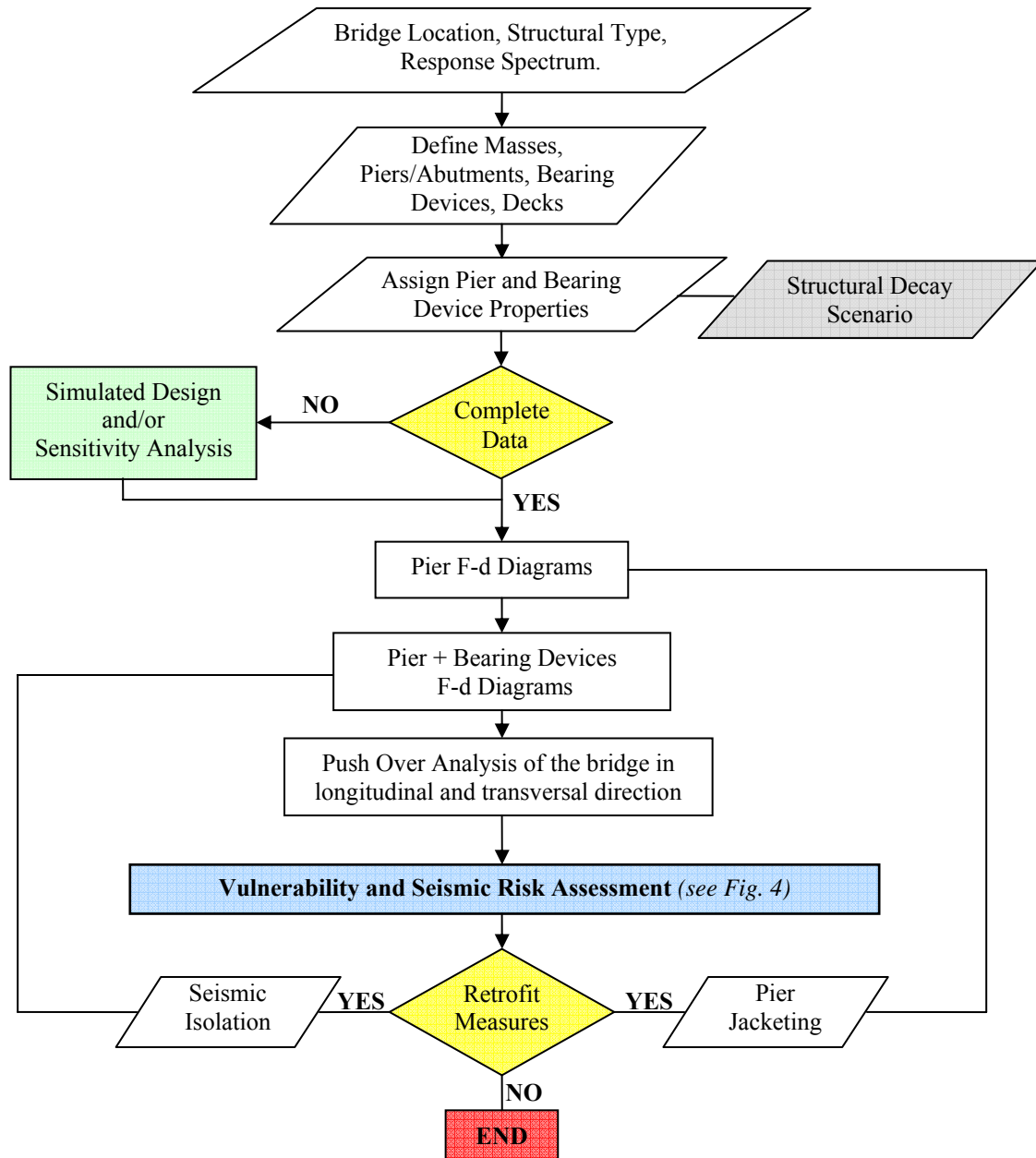


Figure 1: Flowchart of the proposed procedure.

A routine for managing situations of data incompleteness is being implemented. It will adopt two different strategies: simulated design (when the reinforcement of the piers is unknown) or sensitivity analysis (when the characteristics of the bearing devices are unknown).

For a comprehensive description of the procedure reference can be made to [5]. Herein, the most important aspects are briefly presented.

Table 1 shows, for each bridge component, the considered types and the basic modelling assumption of the procedure. As can be seen, deck, foundations and abutments are considered infinitely rigid and resistant. Piers are modelled as elastic beams with plastic hinges at the ends. The mechanical behaviour of the plastic hinges is based on a moment-curvature analysis of the critical sections of the pier. Bearing devices, cable restrainers and shear keys are modelled by link elements with nonlinear force-displacement behaviour (see Fig. 2).

| Component | Types | Modelling Assumptions | Damage states |
|----------------------------------|-----------------------------------------------------------------------------------------------------------------------------------------------------|----------------------------------------------------------------------------------------------------------------------------------------------------------------------------------------------------------------------------------------------------------------------|------------------------------------------------------------------------------------------------------------------------------------------|
| Foundations/ Abutments | - | Infinitely rigid and resistant. | - |
| Deck | Simply supported, Continuous, Gerber, Frame (monolithic). | Diaphragm behaviour. Mass lumped at the bearings based on tributary areas. | - |
| Piers | Single shaft, Simple portal, Double portal, Simple frame, Inter- connected frame, Simple wall, Double wall. | Beam with plastic hinges at the ends. Flexural strength and ductility based on moment-curvature analysis of the sec- tion. Shear strength, material decay, lap-splice effects, instability of longitu- dinal bars and P- Δ effects considered. | Plastic hinge forma- tion. Ultimate rota- tion capacity. Shear failure. Lap-splice failure. Buckling of reinforcing bars. |
| Pier-deck connections | Monolithic, Movement joints. | Link elements modelling bearing devices, cable restrainers (long. direc- tion) and shear keys (trans. direction). | Failure of bearing devices and/or cable restrainers and/or shear-keys. |
| Bearing/ isolation devices | Steel hinge, Steel roller, Neoprene pads, RC/steel pendulum, Steel-PTFE sliders. Rubber-, Steel- and SMA-based isolation systems. | Mechanical behaviour described by nonlinear F-d relationships. Post-failure pier-deck sliding. | Device failure. Post- failure sliding. Ultimate displace- ment capacity. Span unseating. |
| Retrofit measures | Seismic isolation. | Link elements with nonlinear F-d behaviour. | - |
| | Pier Jacketing. | Enhanced ultimate concrete compression strain and shear strength. | - |

Table 1: Types of bridge components and basic modelling assumptions considered in the procedure.

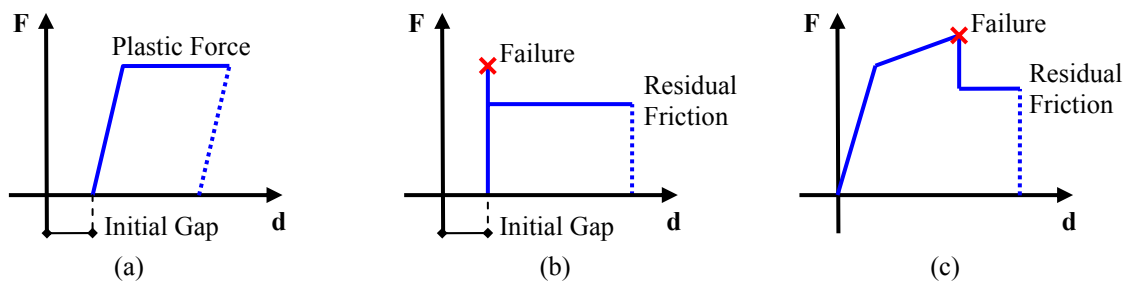


Figure 2: Nonlinear force-displacement behaviour of (a) cable restrainer (longitudinal direction), (b) shear key (transverse direction) and (c) typical bearing device.

The pushover analysis is carried out in the longitudinal and transverse direction separately. First of all, independent pushover analyses of each pier are performed, in which the top-displacement is increased, tracking the formation of plastic hinges up to their ultimate rotation capacity or the attainment of the pier shear strength (see Fig. 3(a)). Lap-splices and buckling effects are also considered (see Fig. 3(b)).

The force-displacement relationship of each pier-bearings system is then derived, by summing up the displacements of pier and bearings under the same horizontal force. Once the lateral force-displacement behaviour of each pier-bearings system has been identified, the response of the bridge in the considered direction (longitudinal or transverse) is examined.

The pier-bearings systems are represented by simple inelastic springs with effective stiffness equal to the secant stiffness at the current displacement. During the pushover analysis, the displacement of stiffness centre of the deck is step-by-step increased. At each step, the spring displacements and associated forces are computed. The effective stiffness of the springs and the position of the centre of stiffness are then updated and a new step of analysis is performed.

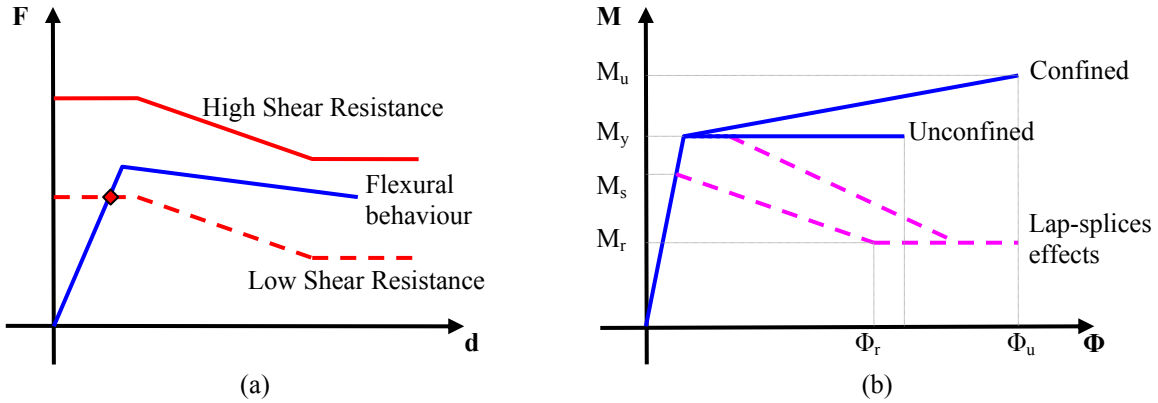


Figure 3: Modelling of flexural plastic hinges: effects due to (a) shear strength, (b) concrete confinement and lap-spliced failure.

The methodology for the evaluation of the seismic vulnerability and seismic risk of bridge structures is schematically summarised in Fig 4. The starting point is represented by the push-over curves of the nonlinear MDOF model of the bridge obtained in the previous phase of the analysis.

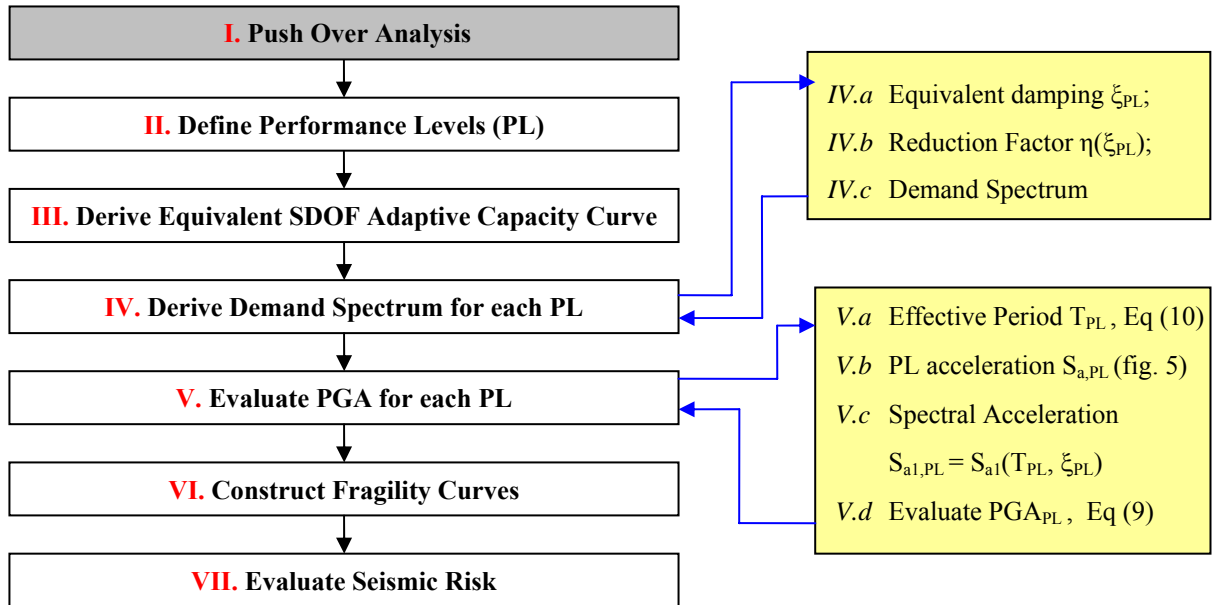


Figure 4: Methodology for the evaluation of the seismic vulnerability and risk of bridges.

As a preliminary step, a number of Performance Levels (PLs) (i.e. damage states), for which seismic vulnerability and seismic risk will be evaluated, are selected. The PLs are automatically defined on the force-displacement curve of each structural member (piers and bearing devices), based on predetermined values of the ratio d/d_y . Five damage states are identified for the piers and three for the bearing devices [5]. During the pushover analysis, the

displacements of each structural member are monitored. As soon as a given damage state is reached in the first structural member, a point is determined on the pushover curve and a new damage state considered in the continuation of the analysis. More detailed information on the definition of the PLs can be found in [5].

The third step of the method (see Fig. 4) is to convert the pushover curve of the nonlinear MDOF model of the bridge into the so-called Capacity Spectrum of the structure [4], i.e. a plot of the displacements and acceleration of an equivalent SDOF model. In the proposed method, the approach recently presented by Casarotti et al. [6] has been followed to convert the pushover curve into an equivalent SDOF adaptive capacity curve. The Equivalent SDOF Adaptive Capacity Curve is step-by-step derived by calculating the equivalent system displacement $S_{d,k}$ and acceleration $S_{a,k}$ based on the actual deformed shape of the bridge at each analysis step k , according to equations (1) and (2), where $V_{b,k}$ is the total base shear of the system, $m_{j,k}^*$ the participating mass of the j -th pier-deck sub-assembly [5], $D_{j,k}$ the horizontal displacement of the j -th pier-bearings system at the analysis step k and $M_{e,k}$ the effective mass of the bridge as a whole, calculated according to equation (3).

$$S_{d,k} = \frac{\sum_j m_{j,k}^* D_{j,k}^2}{\sum_j m_{j,k}^* D_{j,k}} \quad (1)$$

$$S_{a,k} = \frac{V_{b,k}}{M_{e,k} g} \quad (2)$$

$$M_{e,k} = \frac{\sum_j m_{j,k}^* D_{j,k}}{S_{d,k}} \quad (3)$$

As noted by Casarotti et al. [6], the aforesaid approach can be viewed as an adaptive variant of the CSM method, because all the equivalent SDOF quantities, even though formally identical to the corresponding modal quantities, are calculated step-by-step, based on the current deformed shape of the bridge, rather than on invariant elastic modal shape, as in traditional CSM.

The fourth step of the method (see Fig. 4) is to determine the seismic demand associated to each PL. Similarly to CSM, in the proposed method the demand of the expected earthquake ground motion is defined by highly damped acceleration-displacement elastic response spectra. The determination of the demand spectra hence requires the evaluation of the equivalent viscous damping of the bridge associated to each PL. To this end, the following routine has been implemented: (i) choose a given PL, (ii) go back to the pushover database and determine the actual displaced shape of each structural member (piers and bearing devices), (iii) evaluate the equivalent damping of each structural member, based on the Jacobsen's equation [5], specialised to the actual mechanical behaviour of each structural member (see Eqs. (4)-(5)), (iv) combine the contributions of each structural member to get the equivalent viscous damping of the bridge as a whole (see Eqs. (6)-(7)).

The equivalent damping of the bearing devices is calculated based on the following equation:

$$\xi_{b,j} = \frac{E_{visc} + E_{hyst} + E_{fr}}{2\pi \cdot F_{PL} \cdot d_{PL}} \quad (4)$$

in which E_{visc} , E_{hyst} and E_{fr} indicate the energy loss in the device, through its viscous, hysteretic or frictional behaviour, in a cycle of amplitude d_{PL} , being d_{PL} the displacement of the device at the considered PL and F_{PL} the corresponding force level.

As far as piers are concerned, reference has been made to the following relationship:

$$\xi_{p,j} = \xi_0 + \xi_{eq} = 0.05 + \frac{1}{\pi} \left(1 - \frac{(1-r)}{\sqrt{\mu}} - r\mu \right) \quad (5)$$

which relates the equivalent hysteretic damping of the pier (ξ_{eq}) to its displacement ductility μ . The aforesaid relationship has been derived by Kowalski et al. [7], by applying the Jacobsen's approach to the Takeda degrading-stiffness-hysteretic model. In Eq. (5), r is the strain-hardening ratio of the pier force-displacement curve. A viscous damping $\xi_0 = 5\%$ is assumed.

The equivalent damping of each pier-bearings system is then computed, by combining the damping values of pier and devices in proportion to their individual displacements:

$$\xi_j = \frac{\xi_{b,j} d_{b,j} + \xi_{p,j} d_{p,j}}{d_{b,j} + d_{p,j}} \quad (6)$$

Finally, the equivalent damping values of the pier-bearings systems are combined to provide the total equivalent damping of the bridge. The approach followed in the proposed method is to weigh the damping values of the single pier-bearings systems in proportion to the force acting in each of them:

$$\xi = \frac{\sum_{j=1}^n \xi_j F_j}{\sum_{j=1}^n F_j} = \frac{\sum_{j=1}^n \xi_j F_j}{V} \quad (7)$$

Once the equivalent damping of the bridge at each PL is determined, the corresponding demand spectra is derived from the 5%-damped normalized response spectrum defined at the beginning of the analysis (see Fig. 1), by means of proper damping reduction factors $\eta(\xi)$. The reduction factor to be used is selected by the designer among four different relationships, having the general form:

$$\eta = \alpha \sqrt{\frac{a}{(b + \xi)}} \quad (8)$$

For more detailed information on this subject reference can be made to [5].

The fifth step of the method (see Fig. 4) is to find the PGA associated to each PL. From a graphical point of view, this can be done by a translation of the normalised demand spectrum to intercept the capacity spectrum in the performance point (see Fig. 5). From an analytical point of view, the PGA associated to each PL can be determined as the ratio between the acceleration of the capacity curve S_a^* corresponding to each PL (see Fig. 5) and the spectral acceleration at the effective period of vibration T^* associated to each PL, derived from the over-damped normalised response spectrum (see Fig. 8):

$$PGA_{PL} = \frac{S_a^*}{S_{a1}(T^*, \xi)} \quad (9)$$

being:

$$T^* = 2\pi \sqrt{\frac{M^*}{K^*}} = 2\pi \sqrt{\frac{S_d^*}{g \cdot S_a^*}} \quad (10)$$

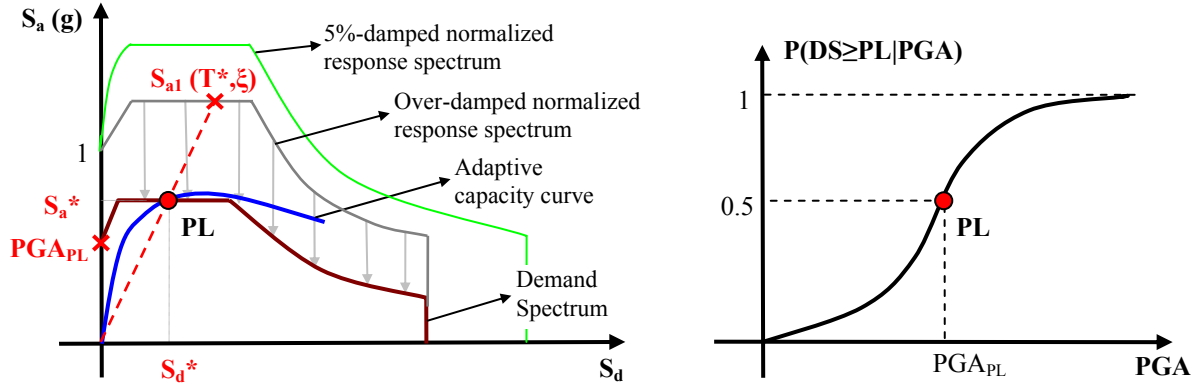


Figure 5: (Left) Evaluation of the PGA associated to a selected PL and (right) corresponding fragility curve.

The PGA values thus obtained represent an estimate of the median threshold value of the peak ground acceleration associated to each performance level. Starting from these values, a series of fragility curves are produced, one for each PL. The fragility curve of each PL provides the probability of exceedance of that PL, as a function of the PGA of the expected ground motion. In line with other similar proposals [8], in the proposed method fragility curves are expressed by a lognormal cumulative probability function:

$$P(DS \geq PL | PGA) = \Phi \left[\frac{1}{\beta_c} \ln \left(\frac{PGA}{PGA_{PL}} \right) \right] \quad (11)$$

in which $P(\cdot)$ is the probability of the Damage State (DS) being equal to or exceeding the selected Performance Level (PL) for a given seismic intensity (PGA), Φ is the standard normal cumulative probability function, PGA_{PL} the median threshold value of the seismic intensity associated to the selected PL (see Eq. (10)) and β_c the total lognormal standard deviation which takes into account the uncertainties related to the input ground motion, bridge response, etc.. According to previous studies [8], a value of β_c equal to 0.6 has been assumed in this method.

The last step of the method consists in the evaluation of the seismic risk through the use of hazard maps, which provide the PGA values at the bridge site having a given probability of exceedance (e.g. 10%) in a given interval of time (e.g. 50 years). The measure of the seismic risk for the bridge under consideration is then given by the probability of exceedance of a given PL conditioned to the local return period hazard.

If needed, at the end of the analysis, retrofit measures can be adopted. In the current version of the procedure, two different seismic retrofit techniques have been implemented (see Fig. 1), namely: (i) seismic isolation [1], realised by substituting the existing bearing devices with proper isolation devices or systems (see Tab. 1) and (ii) confinement of pier through steel, concrete or composite-materials jackets [1].

3 COMPARISON WITH TIME-HISTORY ANALYSES

As a preliminary verification, the proposed procedure has been applied to a number of existing bridges. In order to evaluate the reliability and accuracy of the assessment procedure, the predictions of the method have been compared with the results of Nonlinear Time-History Analyses (NTHAs). The NTHAs have been carried out with the finite element program SAP2000-Nonlinear [9], using 7 different accelerograms, compatible with the response spectrum adopted in the numerical procedure. For each PL, the accelerograms have been scaled to the median threshold value of PGA associated to that PL, as obtained from the proposed procedure (see Eq. (9) and Fig. 5).

In this paper the transverse response of two simply supported span viaducts is examined. The viaducts differ in the pier types (RC frame and RC wall, respectively) and bearing types (steel hinges and neoprene pads, respectively). The comparison between procedure predictions and NTHA results has been carried out in terms of maximum base-shear (V) and maximum displacement of the centre of mass of the deck (D_{CM}).

3.1 Viaduct No. 1

The first viaduct is a 4-span simply supported bridge of 135m total length. The deck is supported by 3 frame-type piers (besides 2 abutments), characterised by 5 RC columns with 1.2m diameter circular cross section and 3.2m effective height. The longitudinal reinforcement ratio of each column is equal to 0.44%. The transverse reinforcement is realised by 10mm diameter hoops at 20mm spacing. The bearing devices are realised through steel elements acting as a pendulum in the longitudinal direction and as a fixed hinge in the transversal direction. The yield strength of the reinforcing steel (type AQ50-60) is equal to 270 N/mm². As far as concrete is concerned, a compression strength of 35 N/mm² has been assumed, based on the design data available.

Figure 6 shows the pushover curve of the viaduct in the transverse direction, as obtained from the proposed procedure. For simplicity, the analysis has been carried out on a single stand-alone span (2 piers only), considered to be completely separated from the adjacent spans at the movement joints. The inelastic behaviour of the structure shown in Fig. 6 is characterised by the development of flexural plastic hinges in the piers, while the bearings remain elastic. The fragility curves associated to the five PLs of the piers are also shown in Fig. 6. Table 2 summarises the values of displacement, effective period, effective damping and PGA provided by the procedure for each PL. The values of PGA reported in the last column of Tab. 2 have been used to scale the accelerograms used in the NTHAs.

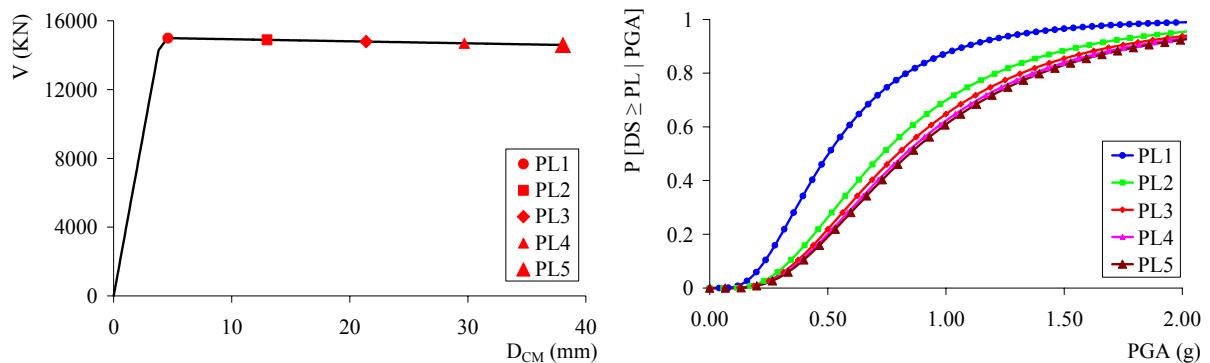


Figure 6: Viaduct no.1: Pushover curve (left) and Fragility curves (right) for different PLs.

| PLs | D_{CM} (mm) | T^* (sec) | ξ (%) | PGA (m/s ²) |
|-----|---------------|-------------|-----------|-------------------------|
| PL1 | 4.65 | 0.134 | 5.00 % | 4.93 |
| PL3 | 21.38 | 0.291 | 24.95 % | 7.81 |
| PL5 | 38.05 | 0.391 | 29.26 % | 8.30 |

Table 2: Viaduct no.1: PGA values corresponding to different PLs, as obtained from the proposed procedure.

A finite element model of the bridge has been developed with SAP2000_Nonlinear. Pier columns have been modelled through beam elements with plastic hinges at the top and the bottom of each column. The cyclic behaviour of the plastic hinges has been described through mul-

tilinear Takeda degrading hysteretic link elements [9]. In the analyses, the numerical parameters α and β , which locate the pivot points for unloading to zero force and reloading from zero force [9], have been taken equal to 0.3-0.2 and 1.5, respectively. The force-displacement behaviour of the bearing devices has been modelled through rigid perfectly plastic link elements [9].

Figure 7 compares the pushover curve provided by the procedure with the cyclic behaviour of the bridge obtained from NTHAs, at different seismic intensities (PGA). The ground acceleration profile of the NTHAs shown in Fig. 7 is always the same, while PGA progressively increases from PGA_{PL1} to PGA_{PL5} (see Tab. 2). The two points marked on the pushover curves emphasise the expected maximum displacement for each PL.

In Table 3 the maximum displacements obtained from NTHAs under different ground motions are reported. For each PL, the average maximum displacement provided by SAP2000 ($AV_{D_{CM}}$) is compared to that predicted by the proposed method ($EX_{D_{CM}}$). The comparison points out an excellent accordance between “actual” and expected performances, with percent differences lower than 15% in the elastic field and limited to a few percents only in the inelastic range.

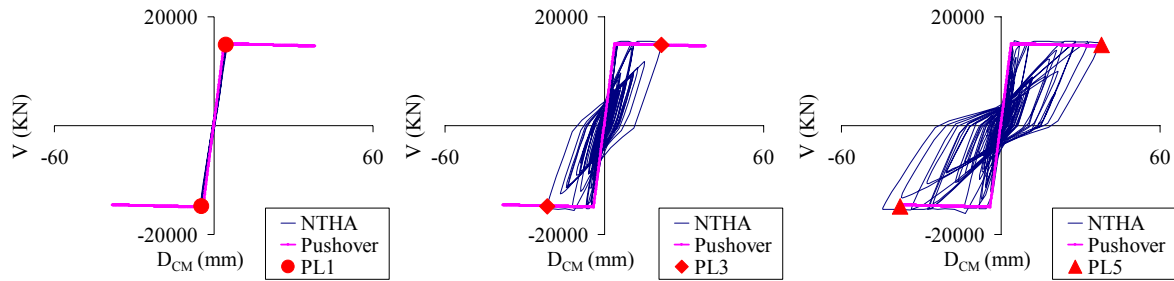


Figure 7: Comparison between expected response (PL_i) and force-displacement curves obtained from NTHAs.

| PL | D_{CM1} (mm) | D_{CM2} (mm) | D_{CM3} (mm) | D_{CM4} (mm) | D_{CM5} (mm) | D_{CM6} (mm) | D_{CM7} (mm) | $AV_{D_{CM}}$ (mm) | $EX_{D_{CM}}$ (mm) | Err (%) |
|-----|-------------------|-------------------|-------------------|-------------------|-------------------|-------------------|-------------------|-----------------------|-----------------------|------------|
| PL1 | 5.57 | 5.08 | 5.56 | 5.59 | 5.36 | 5.63 | 5.42 | 5.45 | 4.65 | - 14.68 % |
| PL3 | 21.21 | 22.86 | 22.39 | 19.04 | 21.87 | 20.64 | 24.91 | 21.85 | 21.38 | -2.15 % |
| PL5 | 41.89 | 51.25 | 38.1 | 44.42 | 31.52 | 30.51 | 34.32 | 38.86 | 38.05 | -2.08 % |

Table 3: Comparison between the displacements predicted by the procedure and those obtained from NTHAs.

3.2 Viaduct No. 2

The second viaduct is a 2-span simply supported bridge of about 70m total length. The deck is supported by a wall-type pier placed in the middle and two lateral abutments. The RC wall pier has a 25m length by 1.2m width rectangular cross section and an effective height of 6.3m. The reinforcement of the wall is made of two grids, with 24mm diameter vertical bars spaced at 330mm and 16mm diameter horizontal bars spaced at 330mm. The grids are connected by 4 cross ties per unit of area of 10mm diameter. The deck is supported by 6 300x600x45mm neoprene pads placed on the abutments and 6 300x600x38mm neoprene pads placed on the pier. The yield strength of the reinforcing steel (type AQ50-60) is equal to 270 N/mm². As far as concrete is concerned, a compression strength of 35 N/mm² has been assumed, based on the design data available.

Figure 8 shows the pushover curve of the viaduct in the transverse direction, as obtained from the proposed procedure. For simplicity, the analysis has been carried out on a single stand-alone span (1 pier + 1 abutment), considered to be completely separated from the adjacent span at the movement joint. The pushover curve of the structure, shown in Fig. 8, basically reproduces the mechanical behaviour of the bearing devices, due to the high transverse

stiffness of the pier. The first selected performance level (PL1 in Fig. 8) corresponds to the occurrence of sliding between deck and pier bearings, for a shear strain in the neoprene pads of the order of 100%. In the analyses, the friction coefficient between neoprene and concrete surfaces has been taken equal to 70%. PL2 corresponds to 50% maximum gap available before sliding between deck and pier (PL3). The unseating of the deck takes place at PL4.

Fig. 8 also shows the fragility curves associated to the PLs selected. For brevity, herein the attention is focused on two PLs only, whose results are summarised in Table 4. The values of PGA reported in Tab. 4 have been used to scale the accelerograms adopted in the NTHAs.

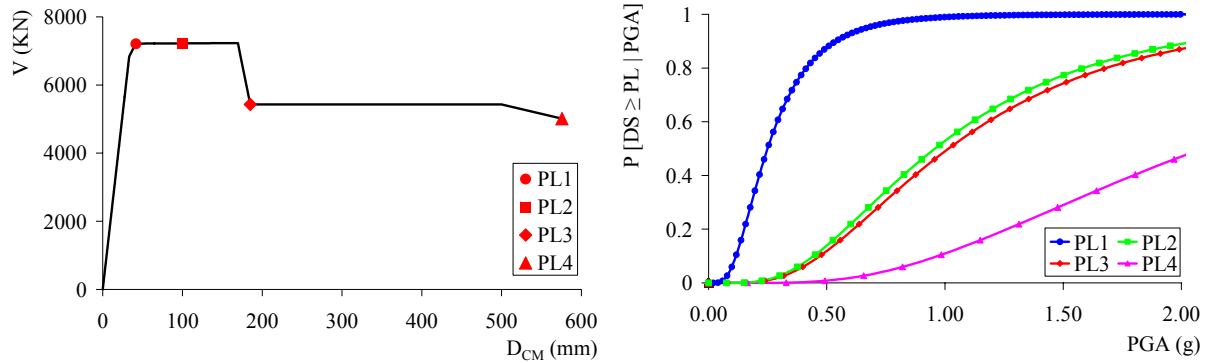


Figure 8: Viaduct no.2: Pushover curve (left) and Fragility curves (right) for different PLs.

| PLs | D_{CM} (mm) | T^* (sec) | ξ (%) | PGA (m/s^2) |
|-----|---------------|-------------|-----------|-----------------|
| PL1 | 34.5 | 0.489 | 6 % | 2.446 |
| PL2 | 100 | 0.819 | 39.49 % | 9.392 |

Table 4: Viaduct no.2: PGA values corresponding to different PLs, as obtained from the proposed procedure.

Figure 9 compares the pushover curve provided by the procedure with typical cyclic behaviours of the bridge, as obtained from NTHAs for the PGA levels reported in Tab. 4. In Table 5 the average maximum displacement obtained from NTHAs ($AV_{D_{CM}}$) is compared to that predicted by the method ($EX_{D_{CM}}$). The comparison confirms the excellent agreement between “actual” and expected behaviour, with percent differences lower than 10%.

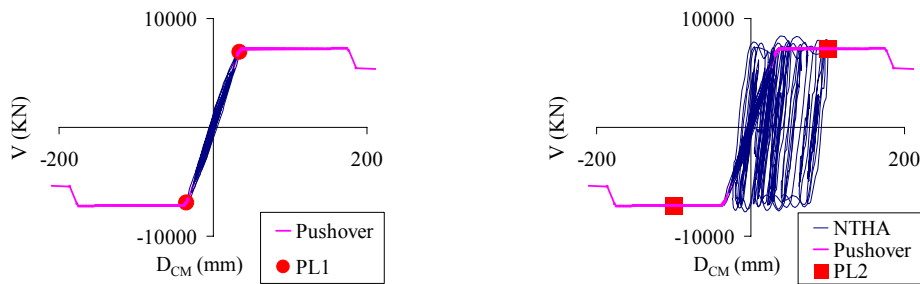


Figure 9: Comparison between expected response (PL_i) and force-displacement curves obtained from NTHAs.

| PL | D_{CM1} (mm) | D_{CM2} (mm) | D_{CM3} (mm) | D_{CM4} (mm) | D_{CM5} (mm) | D_{CM6} (mm) | D_{CM7} (mm) | $AV_{D_{CM}}$ (mm) | $EX_{D_{CM}}$ (mm) | Err (%) |
|-----|----------------|----------------|----------------|----------------|----------------|----------------|----------------|--------------------|--------------------|----------|
| PL1 | 34.92 | 34.5 | 35.28 | 32.35 | 36.82 | 34.21 | 36.86 | 34.99 | 34.5 | - 1.40 % |
| PL2 | 104.31 | 116.45 | 119.4 | 112.03 | 102.26 | 112.27 | 101.68 | 109.77 | 100 | - 8.90 % |

Table 5: Comparison between the displacements predicted by the procedure and those obtained from NTHAs.

4 CONCLUDING REMARKS AND FUTURE DEVELOPMENTS

A numerical procedure for the seismic assessment of existing bridges has been presented. It is inspired to the principles of the Capacity Spectrum Method, reviewed under an “adaptive” perspective. The procedure relies on accurate models and a suitable algorithm for push-over analysis. A series of fragility curves are created at the end of the procedure, which describe the seismic vulnerability of the bridge from a probabilistic point of view. The seismic risk of the bridge is expressed in terms of probability of exceedance in 50 years of given damage states, conditioned on the site seismic hazard.

The procedure allows to evaluate the vulnerability and seismic risk of the structure in different conditions: (i) as-built, (ii) taking account of the current structural decay, (iii) taking account of the natural evolution of the decay process and programmed maintenance and/or seismic upgrading measures.

As a preliminary verification, the proposed procedure has been applied to a number of existing bridges and the results compared to those provided by nonlinear time-history analyses. The comparisons shown in the paper, though limited to two bridges only, have shown an excellent accordance between “actual” and expected performances.

Work is still in progress and additional numerical and experimental studies are being carried out, in order to further verify and improve the procedure.

5 ACKNOWLEDGEMENTS

This work has been partially funded by Autostrade per l'Italia SpA, within the framework of the SAGGI research project, funded by the Italian Ministry for the University and the Research (MUR) and led by Autostrade per l'Italia SpA.

REFERENCES

- [1] M.J.N. Priestley, F. Seible, G.M. Calvi, *Seismic Design and Retrofit of Bridges*, John Wiley & Sons, 1996.
- [2] Ordinanza No. 3274/2003 e 3431/2005 del Presidente del Consiglio dei Ministri, Roma.
- [3] M.J.N. Priestley, G.M. Calvi, Direct displacement-based seismic design of concrete bridges. *Proc. V ACI International Conf. of Seismic Bridge Design and Retrofit for Earthquake Resistance*, December 8-9, 2003 - La Jolla, California.
- [4] S.A. Freeman, Development and use of capacity spectrum method. *Proc. 6th U.S. National Conference in Earthquake Engineering*, Seattle (USA), 1998.
- [5] M. Dolce, D. Cardone, G. Perrone, Seismic risk assessment of highway bridges. *Proc. 1st US-Italy Seismic Bridge Workshop*, Pavia, April 18-20, 2007.
- [6] C. Casarotti, R. Pinho, G.M. Calvi, An adaptive capacity spectrum method for assessment of bridges subjected to earthquake action. *Proc. 1st ECEES Congress*, Geneva, 2006.
- [7] Kowalsky MJ, Priestley MJN, MacRae GA. Displacement-based design of RC bridge columns in seismic regions. *Earthquake Engineering and Structural Dynamics*, 1995; 24(12):1623–1643.
- [8] A. Kappos, I. Moshonas, T. Paraskeva, A. Sextos, A Methodology for derivation of seismic fragility curves for bridges with the aid of advanced analysis tools, *Proc. 1st ECEES Congress*, Geneva, 2006.
- [9] Computer and Structures, inc., *SAP2000 Advanced: Static and Dynamic Analysis Finite Element Analysis of Structures*, University Ave. Berkeley, CA, 2005.